

**MINISTRY OF EDUCATION
AND TRAINING**

**VIETNAM ACADEMY OF
SCIENCE AND TECHNOLOGY**

**GRADUATE UNIVERSITY OF SCIENCE AND
TECHNOLOGY**



PHAM LE KHUONG

**APPLICATION OF RADIO WAVE DATA AND
NUMERICAL MODEL TO RESEARCH AND
EVALUATE SOME ATMOSPHERIC PARAMETERS IN
SOME AREAS OF VIETNAM**

**SUMMARY OF DISSERTATION ON MATERIAL
SCIENCE**

Major: Geophysics

Code: 9 44 01 11

Hanoi- 2025

The dissertation is completed at: Graduate University of Science and Technology - Vietnam Academy Science and Technology.

Supervisors:

1. Supervisor 1: Dr. Nguyen Xuan Anh, Institute of Earth Sciences
2. Supervisor 2: Dr. Nguyen Van Hiep, Northern Regional Hydro-Meteorological Center

Referee 1: Prof. Dr. Phan Van Tan

Referee 2: Assoc. Prof. Dr. Nguyen Viet Lanh

Referee 3: Dr. Du Duc Tien

The dissertation is examined by Examination Board of Graduate University of Science and Technology, Vietnam Academy of Science and Technology at (time, date.....)

The dissertation can be found at:

1. Graduate University of Science and Technology Library
1. National Library of Vietnam

INTRODUCTION

Reason for choosing topic: The temperature, pressure, humidity are the basic parameters of the atmosphere. Determining these parameters in a certain area is important which help us to determine the state of the atmosphere, weather and climate conditions in that area. This are basic and important parameters used in weather and climate forecasting. In addition, determining these parameters is also important for other field such as: economic and social development, serving in national security and defense, natural disaster mitigation, satellite data correction, reducing errors in positioning and radio navigation and many other field. This atmospheric parameters can be determined by many different methods: direct measurement methods, remote sensing methods or can be determined by using numerical models.

Remote sensing methods using radio wave data to determine atmospheric parameters have showed their superiority and increasingly used. The method of using low-orbit satellites (LEO) to observe the Earth's atmosphere is one of them. This method uses radio occultation (RO) techniques to determine the profile of atmospheric parameters (temperature, relative humidity, absolute humidity, pressure, water vapor pressure, atmospheric refractive index) from radio wave data (transmitted from GPS satellites to LEO satellites). This observation data is commonly referred to as GPSRO data. GPSRO data has similar characteristics to radiosonde data. The advantage of these method is the ability to provide atmospheric parameter profiles on global scale. The GPSRO data has become an important data source, especially in oceanic and polar regions where there is very little the atmospheric profile observations.

Another method using radio waves to probe the atmosphere that is widely used in the world is the method using global positioning system (GNSS) data collected at the surface. This method determines the zenith troposphere delay (ZTD) and total precipitable water (TPW). It has become an important source of atmospheric observation data in weather and climate research and forecasting because the number of GNSS receivers on the

ground is increasing. This data can be used to monitor the change of total precipitable water in near real time or assimilated into numerical forecasting models.

In our country, profile of atmospheric parameters are mainly observed and measured through a network of radiosonde stations. These parameters are observed from 1 time/day to 2 times/day. The network of radiosonde stations in Vietnam includes 6 stations, they are mainly located on the mainland (5 stations) and 01 station is located on a coastal island. Thus, the monitoring data of radiosonde stations is very little or almost non-existent in the East Sea area. Therefore, GPSRO data has become an important source of high-altitude atmospheric monitoring data to supplement radiosonde data in the Vietnam area and especially in the East Sea area. However, the assessment of the quality and application of this data in atmospheric and weather research in the Vietnam area has not received much attention from scientists. In addition, the number of GNSS receive stations installed at the ground is increasing in our country. The amount of data collected is increasing. However, the application of this data in atmospheric, weather and climate research is still limited. Some scientists have used this data to calculate TPW at some times of the day and study the law of TPW change. Calculating TPW with minute resolution and studying the change of TPW in some weather phenomena has not studied in Vietnam. On that basis, the doctoral student (NCS) chose the topic "**Application of radio wave data and numerical model to study and evaluate some atmospheric parameters in some areas of Vietnam**".

Objective of the dissertation: The study evaluates the ability to observe, the quality and characteristics of some atmospheric parameters (atmospheric refractive index, humidity, temperature) in some areas of Vietnam using radio wave data and WRF model; The study applies radio wave data sources and WRF model simulation of atmospheric parameters to study some extreme weather phenomena in some areas of Vietnam.

Contents of the dissertation: (1) A overview study of radio observation methods, model calculations, and evaluation of related

atmospheric parameters. (2) Research on methods of using radio wave data (GPSRO and surface GNSS data) and WRF model products to calculate some atmospheric parameters. (3) Evaluating wetPf2 data and GNSS data in the Vietnam region by comparing them with other sources such as radiosonde data, Aeronet data, and model products. (4) Using wetPf2 data to study the thermal and humid characteristics of maritime air masses over the East Sea region (represented by the Hoang Sa Islands and Truong Sa Islands). Application of wetPf2 data analyze the structure of atmospheric fields under extreme weather conditions (typhoons) in the East Sea region and neighboring areas. (5) Using GNSS data to calculate atmospheric total precipitable water with high temporal resolution (1-minute intervals), and applying the results to study diurnal variation and temporal changes of total precipitable water. The calculated results and model simulation outputs are then used to investigate the variation of total precipitable water associated with cold air in the Nghia Do area.

New contributions of the dissertation: (1) Clarified the quality of wetPf2 data in Vietnam and neighboring regions. Clearly analyzed the variation characteristics of temperature and relative humidity fields representing the northern East Sea (Hoang Sa Islands area) and the southern East Sea (Truong Sa Islands area), as well as the anomalous structures of some atmospheric fields under extreme weather conditions (typhoons) in the East Sea and neighboring areas. Calculated and evaluated the reliability of total precipitable water with 1-minute resolution, and identified the diurnal variation and characteristics of total precipitable water changes associated with cold air based on GNSS data in the Nghia Do area.

CHAPTER 1. OVERVIEW OF THE USE OF RADIO WAVE DATA AND NUMERICAL MODELS IN ATMOSPHERIC RESEARCH

1.1. Overview of the use of radio wave data for studying and assessing atmospheric parameters

1.1.1. Overview of international research studies

With the rapid development of technology, the radio occultation (RO) method and the use of ground-based Global Navigation Satellite

System (GNSS) receivers for atmospheric monitoring are among the non-traditional observation methods that have been widely used around the world. This method was first developed and applied in the Mariners 3 and 4 missions in the 1960s (Yunck, 2002). In 1995, it was applied in the GPS/MET project (Ware et al., 1996). Since then, this method has been applied in many projects such as SAC-C (Schmidt et al., 2005), GRACE (Beyerle et al., 2005), COSMIC/FORMOSAT-3 (Anthes et al., 2008), MetOp (Gorbunov et al., 2011). Most recently, the RO technique has been used for radio wave signal processing in the COSMIC-2/FORMOSAT-7 mission (Schreiner et al., 2020). This method has been extensively studied and its reliability evaluated by many researchers (Kuo et al., 2005; Xu et al., 2009; Zhang et al., 2011; Wang et al., 2013; Shao et al., 2021; Veenus et al., 2022). Data from this method have been used to study the thermal structure in typhoons (Biondi et al., 2013; Rivoire et al., 2016), and to analyze variations in temperature and humidity across various regions (Kuleshov et al., 2016).

The method of determining atmospheric parameters using surface-based GNSS data has attracted the attention of many researchers (Bevis et al., 1992; Karabatic et al., 2011; Ahmed et al., 2014; Gopalan et al., 2021). Data obtained through this method have been evaluated by comparison with radiosonde observations (Tregoning et al., 1998; Baelen et al., 2005; Fernández et al., 2010; Torres et al., 2010) and reanalysis data (Namaoui et al., 2017). One of the widely used GNSS data processing tools today is the CSRS-PPP tool. The reliability of this method has been confirmed through comparisons with IGS data (Guo, 2015; Astudillo et al., 2018; El-Mewafi et al., 2019) or with radiosonde data (Rose et al., 2023). This data is used to study the trends of total water vapor (Nilsson and Elgered, 2008; Torres et al., 2010), for near-real-time monitoring of total precipitable water (Bosy et al., 2012) or in the study some weather phenomena (Kuleshov et al., 2016; Bonafoni and Biondi, 2016; Priego et al., 2017; Rose et al., 2023).

1.1.2. Overview of domestic research studies

Domestic research related to the use of GPSRO and surface-based

GNSS data for atmospheric studies remains limited and underdeveloped. GPSRO data have been used by some Vietnamese researchers to calculate atmospheric convective indices (Nguyen Xuan Anh and Pham Le Khuong, 2008), to determine the refractive index and radio wave propagation conditions in the troposphere over the Hanoi area (Pham Chi Cong et al., 2021), or to assimilate into numerical weather prediction models (Pham Quang Nam et al., 2019). GNSS data for studying tropospheric zenith delay (ZTD) and total precipitable water have not received much attention, and the number of studies in this area is still small (Le Huy Minh et al., 2009; Lai Van Thuy et al., 2022). Existing studies have mainly calculated total precipitable water at certain times of the day and have not yet applied the data for monitoring changes in total precipitable water during weather phenomena.

1.2. Overview of using WRF model to simulate atmospheric parameters

1.2.1. Overview of international research studies

The Weather Research and Forecasting (WRF) model is a mesoscale numerical weather prediction model. WRF is widely used for both operational weather forecasting and research in many countries around the world (Dasari et al., 2014; Pérez-Jordán et al., 2018; Hassanli and Rahimzadegan, 2019; Noh et al., 2021; Ojrzyńska et al., 2022; Zhang et al., 2022).

1.2.2. Overview of domestic research studies

In Vietnam, the WRF model has attracted significant interest from researchers and has been widely used for studying and forecasting various meteorological fields. It has been applied in the simulation and prediction of rainfall fields (Hoang Duc Cuong, 2011; Truong Hoai Thanh et al., 2011; Vu Van Thang et al., 2017; Nguyen Tien Toan et al., 2018; Chu Thi Thu Huong et al., 2018; Du Duc Tien et al., 2019; Vu Van Thang et al., 2019; Truong Ba Kien et al., 2022), temperature field simulations (Do Huy Duong, 2004; Hoang Duc Cuong, 2011; Chu Thi Thu Huong, 2018), and humidity field simulations (Dang Hong Nhu and Nguyen Van Hiep, 2016).

CHAPTER 2. DATA AND RESEARCH METHODS

2.1. Used data

WetPf2 data was collected for a period of 4 years from October 2019 to September 2023 in Vietnam and neighboring areas. Radiosonde data was collected at 3 stations: Lang Station (Hanoi), Da Nang, Tan Son Hoa (Ho Chi Minh City) for a period from October 2019 to September 2023. GNSS data was collected in Nghia Do area for a period from September 22, 2022 to March 31, 2023. Total precipitable water data was collected from AERONET station for a period from September 22, 2022 to March 31, 2023. Temperature and rainfall data was collected from automatic weather station in Nghia Do for a period from September 22, 2022 to March 31, 2023. Storm center location data was collected during the active period of 13 storms in 2020. ECMWF ERA5 reanalysis data was collected for February and April from 1991-2020. NCEP FNL reanalysis data was collected from 22/09/2022 to 31/03/2023. NCEP GFS data was collected during the active period of 13 storms in 2020.

2.2. Research method

2.2.1. Radio Occultation method

An electromagnetic wave signal traveling through the atmosphere is refracted according to Snell's law due to the vertical gradient of atmospheric density, which is expressed as the refractive index. The overall effect of the atmosphere can be characterized by the total bending angle α , the asymptotic ray distance a and the tangent radius r_t . The variation of α with respect to a or r depends on the vertical profile of the atmospheric refractive index $n(r)$. Through an Abelian transformation, $n(r)$ is obtained from the parameters α and a .

$$n(r) = \text{Exp} \left[\frac{1}{\pi} \int_{a_1}^{\infty} \frac{\alpha}{\sqrt{a^2 - a_1^2}} da \right] \quad (1)$$

Then, the temperature, pressure, and steam pressure parameters will be calculated from the $n(r)$ data.

2.2.2. Calculation of total precipitable water from GNSS data

The CSRS-PPP tool is used to calculate the ZTD and ZWD quantities. Subsequently, the total precipitable water is calculated as follows:

$$TPW = ZWD/k \quad (2)$$

Where k is a coefficient calculated using the following empirical formula:

$$k = 461.5 * 10^{-5} * \left[3.719 * \frac{10^5}{T_m} + 16.4221 \right] \quad (3)$$

T_m (K) can be approximated by (Bevis et al., 1992)

$$T_m = 70.2 + 0.72 * T_s \quad (4)$$

T_s (K) is the surface temperature measured by the automatic weather station installed at Nghia Do station. The calculated total precipitable water has a temporal resolution of 1 minute.

2.2.3. Evaluation of atmospheric parameters calculated from radio wave data

2.2.3.1. Evaluation of temperature, relative humidity, and atmospheric refractive index data from wetPf2 data

To evaluate the quality of GPSRO data in atmospheric observation, atmospheric parameters including temperature, relative humidity, and refractive index from the wetPf2 dataset are compared with radiosonde data from 3 stations in Hanoi (Lang), Da Nang, Ho Chi Minh City (Tan Son Hoa). The selection criteria for comparison sample pairs are based on time differences of ≤ 1 hour, ≤ 2 hours, and ≤ 3 hours, and spatial distances of ≤ 100 km, ≤ 200 km, and ≤ 300 km (forming a total of 9 combinations). Once the comparison pairs are selected, the data are interpolated to 10 standard pressure levels (925mb, 850mb, 700mb, 500mb, 400mb, 300mb, 250mb, 200mb, 150mb, 100mb) using the formula (Wang et al., 2013):

$$T = \alpha. T_1 + \beta. T_2 \quad (5)$$

$$RH = \alpha. RH_1 + \beta. RH_2 \quad (6)$$

$$N = \alpha. N_1 + \beta. N_2 \quad (7)$$

$$\alpha = \frac{\ln P - \ln P_2}{\ln P_1 - \ln P_2} \quad (8)$$

$$\beta = \frac{\ln P_1 - \ln P}{\ln P_1 - \ln P_2} \quad (9)$$

Statistical quantities including mean error (ME), standard deviation of the mean error and the correlation coefficient are used to compare the wetPf2 data with radiosonde data.

Additionally, the wetPf2 data are also compared with WRF model simulation data under storm conditions. The wetPf2 values are compared with the nearest grid point values at 10 standard pressure levels, with a time difference of ± 30 minutes. The statistical quantities used in this comparison are ME and standard deviation of errors.

2.2.3.2. Evaluation of total precipitable water data calculated from GNSS data

To evaluate the quality of total precipitable water data calculated from GNSS observations in the Nghia Do area, the results are compared with the daily average total precipitable water product from AERONET data at the Nghia Do station. The GNSS-derived values are also compared with total precipitable water values at 7:00 AM and 7:00 PM (local time) from radiosonde data at the Hanoi (Lang) station, as well as with model simulation results at the nearest grid point. Within the scope of this dissertation, statistical metrics including mean error (ME), mean absolute error (MAE), relative mean absolute error (RMAE), root mean square error (RMSE), and the correlation coefficient are used to compare the GNSS-derived total precipitable water with that from AERONET and radiosonde data.

2.2.4. Research method for studying atmospheric fields during storms

The coordinate data of storm centers with a 6-hour temporal resolution are linearly interpolated to obtain storm center positions at a 1-hour resolution. Data profiles from COSMIC-2 are grouped into 12 categories based on their distance from the storm center to the observation location, with intervals of 100 km. To calculate anomaly values, the profiles of temperature, relative humidity, water vapor pressure, and atmospheric refractivity index are subtracted from the corresponding

monthly mean profiles of these parameters (Biondi et al., 2013; Rivoire et al., 2016). The monthly mean profiles are calculated by averaging each parameter for each month within a $2^\circ \times 2^\circ$ latitude–longitude grid using COSMIC-2 data over a four-year period (10/2019 – 09/2023).

2.2.5. Model Application method

In this dissertation, the Weather Research and Forecasting (WRF) model is used to simulate meteorological fields, which support a clearer analysis of atmospheric conditions during data interpretation. The model includes two nested domains: the outer domain (d01) has a horizontal resolution of 18 km, and the inner domain (d02) has a resolution of 6 km. The parameterization scheme used in the model are based on the study by Truong Ba Kien et al. (2022) including: The microphysical parameterization scheme is the Goddard scheme (7); the convective parameterization scheme is the Kain-Fritsch scheme (1); the planetary boundary layer parameterization scheme YSU (1); the longwave radiation parameterization scheme RRTMG (4); the shortwave radiation parameterization scheme RRTMG (4).

CHAPTER 3. CHARACTERISTICS OF SOME ATMOSPHERIC FIELDS OVER VIETNAM AND NEIGHBORING AREA USING WETPF2 DATA

3.1. Evaluation of wetPf2 data in Vietnam and neighboring areas

The results show that the mean error between the wetPf2 data and the radiosonde data for air temperature ranges from $-0,06^\circ\text{C}$ to $-0,02^\circ\text{C}$, with a standard deviation between $0,73^\circ\text{C}$ and $1,04^\circ\text{C}$ and a correlation coefficients ranging from 0,86 to 0,93. The mean error in relative humidity between the two data sources varies from 11,63% to 12,45%, with a standard deviation ranging from 15,04% to 19,06% and a correlation coefficient between 0,63 and 0,76. The mean error for the atmospheric refractivity index ranges from $-0,92$ to $-0,62$, with an annual average standard deviation between 3,10 and 4,04 and a correlation coefficient from 0,76 to 0,87. The comparison results for air temperature, relative humidity, and atmospheric refractivity index between wetPf2 data and radiosonde

data in the Vietnam region are consistent with studies conducted in other parts of the world. These results confirm that wetPf2 data can be used in atmospheric research and operational weather forecasting in the Vietnam region.

The comparison results between wetPf2 data and WRF model simulations show that the mean error of air temperature and the corresponding standard deviation range from $-0,54^{\circ}\text{C}$ to $0,62^{\circ}\text{C}$ and from $0,38^{\circ}\text{C}$ to $1,29^{\circ}\text{C}$, respectively, at pressure levels $\geq 150\text{mb}$ in 3 forecast periods $< 6\text{h}$, 24h and 48h and 3 distances of 100km , $500\text{-}600\text{km}$ and $1100\text{-}1200\text{km}$ from the typhoon center. For relative humidity, the mean error ranges from $-6,1\%$ to $20,0\%$ with standard deviations generally $\leq 20,3\%$ at pressure levels $\geq 400\text{mb}$ in all cases. Compared to the results obtained from comparisons with radiosonde data, the differences between wetPf2 data and model simulations are not significant.

3.2. Characteristics of some atmospheric fields in the Hoang Sa and Truong Sa islands regions

3.2.1. Characteristics of air temperature field

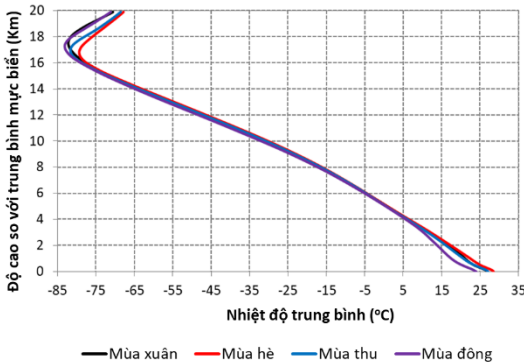


Figure 3.1. Results of the seasonal variation in average temperature over the Hoang Sa islands region. Graphs in black (spring), red (summer), blue (autumn), purple (winter)

From October 2019 to September 2023, a total of 6215 wetPf2 soundings were recorded over the Hoang Sa islands region (13°N - 18°N , 110°E - 115°E). Based on this dataset, the seasonal average temperature profiles (T_m) were calculated for each of the four seasons at various

altitude levels (Fig 3.1). The temperature decreases with height from the surface up to the top of the troposphere (from 16,8 km to 17,5 km). The annual variation of T_m at each level shows a clear pattern, T_m reaches its highest values in summer and lowest in winter. The T_m profiles within the 0km to 3,5km layer exhibit significant seasonal variability. The amplitude of T_m variation at each level ranges from 1,3°C to 5,0°C. This strong seasonal variability in T_m indicates a considerable influence of the winter monsoon on this region.

In the Truong Sa islands region, a total of 7730 wetPf2 soundings were recorded, a higher number compared to the Hoang Sa islands. The vertical variation trend of average temperature (T_m) across the four seasons is similar to that observed in the Hoang Sa islands, decreasing from the surface to the top of the troposphere. Regarding the annual cycle of T_m , within the atmospheric layer from the surface to 2,0 km, summer exhibits the highest T_m values, while winter has the lowest. The seasonal amplitude of T_m at each level ranges from 1,2°C to 2,2°C. Near the surface, T_m value is 26,1°C (in winter) and 28,3°C (in summer). Compared to the Hoang Sa islands, the seasonal temperature variation in the Truong Sa islands is significantly smaller. This indicates a weaker influence of the winter monsoon in this region, resulting in higher winter T_m values and a lower annual temperature variation compared to the Hoang Sa islands.

3.2.2. *Relative humidity field characteristics*

The vertical profile of seasonal average relative humidity (RHm) within the 0 km to 12 km layer over the Hoang Sa islands region, with a height resolution of 50 meters, is shown in Figure 3.2. The results indicate that RHm values are higher in the atmospheric boundary layer than in the free atmosphere. Near the surface, seasonal average humidity values range from 75,4% (summer) to 77,6% (winter). RHm increases with height and reaches a maximum at an altitude of about 0,6 km to 0,7 km. which typically corresponds to the lifting condensation level (LCL). The maximum RHm values are 80,7% (spring), 80,5% (summer), 85,5%

(autumn) and 85,3% (winter). Due to the influence of the winter monsoon, cold air masses carrying lower temperatures from northern Asia reach the East Sea, causing the temperature to approach the dew point. This results in the highest relative humidity values occurring in winter within the layer from the surface up to 400 meters. In the free atmosphere, RHm values during spring, autumn, and winter decrease with height, reaching a minimum in the mid-troposphere, and then increase again at higher altitudes.

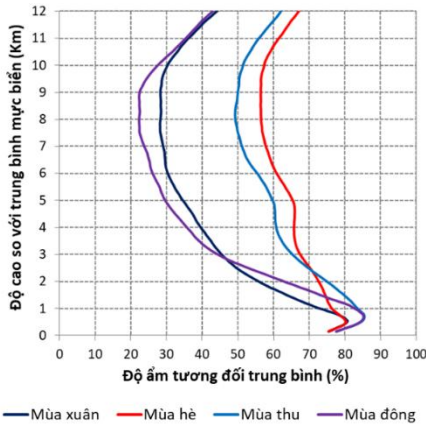


Figure 3.2. Results of average relative humidity changes of four seasons in the Paracel Islands area. Graphs in black (spring), red (summer), blue (autumn), purple (winter)

For the Truong Sa islands region, the results show that the seasonal average relative humidity values range from 74,3% (summer) to 78,5% (winter) in the near-surface layer. Similar to the Hoang Sa islands region, RHm increases with altitude and reaches a peak at around 0.65 km. The peak RHm values are 80,3% (spring), 81,6% (summer), 84% (autumn) and 85,4% (winter). RHm then gradually decreases, reaching a minimum in the mid-troposphere. RHm values in the boundary layer are higher than those in the free atmosphere. Within the layer below 1,25 km, the annual variation amplitude of RHm is relatively small (<7,5%). The seasonal average relative humidity in winter and autumn is higher than in summer and spring. This may be attributed to the influence of the winter monsoon and the activity of the ITCZ (Intertropical Convergence Zone). The winter monsoon transports cooler air to the East Sea, and the ITCZ, with its active

convection zone, shifts toward lower latitudes (closer to or over the Truong Sa islands) during the early winter months. These conditions lead to higher relative humidity levels in the air mass during winter and autumn.

3.2.3. *Differences in temperature and humidity fields between maritime and continental air masses at the same latitude*

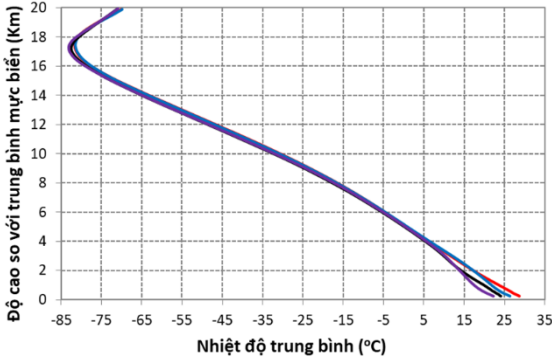


Figure 3.3. Average temperature profile during the hot months (April, May, June) on land (red), at sea (blue) and in winter on land (black), at sea (purple)

To highlight the variation characteristics of temperature and relative humidity fields over the sea, the doctoral candidate conducted a comparison with the variation characteristics of temperature and relative humidity fields between the Hoang Sa islands and the mainland region (13°N - 18°N, 101°E - 106°E). The selected mainland region lies at the same latitude as the maritime area (Hoang Sa islands). Based on surface station temperature statistics, the hottest period across the entire mainland area occurs from late spring to early summer (Senapeng et al., 2022). Therefore, the three-month period of April, May, and June was selected to calculate the average temperature during the hottest months. The winter period (December, January, February) was chosen to examine the temperature of the two air masses during the coldest months.

When comparing the average temperature profiles during the hottest months and the winter season between the Paracel Islands area and the mainland, there is no significant difference in the average temperature variation at higher altitudes (above 3 km). However, at lower altitudes (below 2 km) during the hot months (AMJ), the average temperature of the

air mass over the mainland is 1°C to 2°C higher than that over the sea due to land surface heating (Figure 3.3). This land surface warming during the hot months is clearly reflected in the 30-year long-term average of 2-meter air temperature from ERA5 (ECMWF) data. In February and April, the continental air mass shows significantly higher temperatures compared to the air mass over the Hoang Sa islands region.

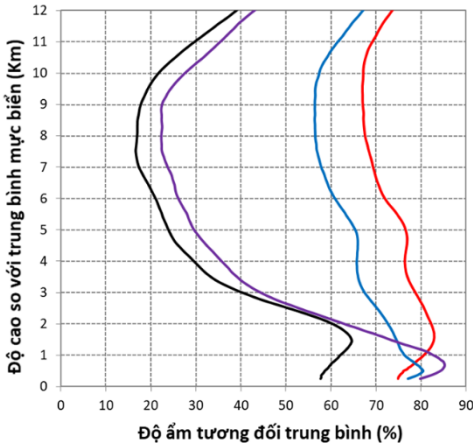


Figure 3.2. Average relative humidity profile (%) in summer (June, July, August) on land (red), on sea (blue) and in winter (December, January, February) on land (black), on sea (purple)

Comparison of average relative humidity values shows that the mean relative humidity (RHm) in both regions is high during the summer season. In the layer below 0,8 km, the marine air mass exhibits higher RHm values than the continental air mass. This may be attributed to the role of turbulent motions, which transport abundant moisture from the sea surface into the planetary boundary layer. However, in the free atmosphere, the average summer RHm of the continental air mass is higher than that over the Hoang Sa islands region (Figure 3.4). This could be due to the influence of the southwest monsoon during summer, which transports moist air masses from the Indian Ocean to the mainland (Khedari et al, 2002). Under the influence of local factors and topography, strong convection develops, carrying moisture to higher levels in the free atmosphere. This may be a key factor leading to higher RHm values over the mainland compared to the sea in the free atmosphere during summer.

In winter, the average relative humidity (RHm) profile shows a significant difference between the two air masses in the planetary boundary layer (below 2 km). The RHm values over the mainland are much lower than those over the Hoang Sa islands region. During this season, the northeast monsoon brings dry and cool air to the area (Khedari et al, 2002). Due to the influence of the dry northeast monsoon, the relative humidity of the air mass in the boundary layer over the mainland is lower compared to that over the Hoang Sa islands. In the free atmosphere, there is no significant difference in relative humidity between the two air masses, although the RHm values over the mainland remain slightly lower than those over the Hoang Sa islands (Figure 3.4)

3.3. Characteristics of some atmospheric fields in the East Sea and neighboring areas during storm activity from wetPf2 data

3.3.1. Temperature field characteristics

The results show that a warm anomaly region exists at altitudes from 2,5 km to 15 km at all distances from the typhoon center to 1200 km. The maximum warm anomaly reaches 1,5°C at altitudes between 6,5 km and 13,5 km within the area less than 100 km from the typhoon center. The temperature anomaly decreases with increasing distance from the storm center, with the area of temperature anomalies $>1^{\circ}\text{C}$ extending up to 600 km away from the storm center. The results also indicate the presence of cold anomaly regions at altitudes below 2,5 km and above 16 km. The cold anomaly below 2,5 km reaches a peak of less than $< -0,5^{\circ}\text{C}$ and extends from the storm center to a distance of approximately 400 km. A stronger cold anomaly ($< -1,0^{\circ}\text{C}$) is observed at altitudes from 16 km to 17,5 km, stretching up to 600 km from the storm center (Figure 3.5). Simulations from the WRF model show that near the storm center, the average vertical wind speed ranges from 0,15 m/s to 1,11 m/s, which is higher than in areas farther from the storm center. The distribution of temperature anomalies aligns with the simulated vertical velocity fields. The spatial distribution of temperature anomalies in this study is also consistent with previous studies using COSMIC data (Rivoire et al., 2016).

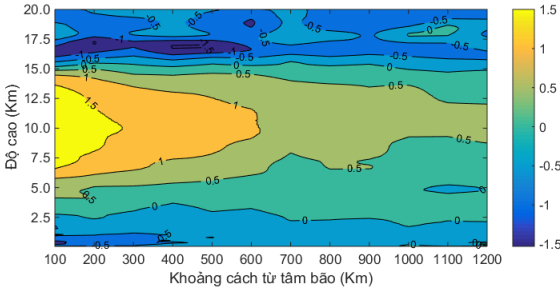


Figure 3.5. Temperature anomalies ($^{\circ}\text{C}$) compared to monthly average values from COSMIC-2 data according to height and distance from the storm center during the storm's movement into the East Sea during the 2020 storm season

3.3.2. Relative humidity field characteristics

The calculation results indicate that under the influence of a typhoon, relative humidity values in the troposphere increase compared to the monthly average. The area with the greatest increase in relative humidity is concentrated within 600 km from the storm center, with the maximum increase exceeding $>25\%$. The region where the relative humidity increases by more than 20% is mainly located at altitudes between 5 km and 12,5 km. In the lower atmosphere below 2,5 km of the area from the storm center to 300 km, the average increase in relative humidity ranges from 5% to 15%. At distances greater than 800 km from the storm center, the increase in relative humidity is significantly smaller compared to areas within 600 km of the center. In these farther regions, the increase in relative humidity is mostly less than 10%, with only a few areas between 7,5 km and 12,5 km showing an increase above 10%.

3.3.3. Characteristics of steam pressure field

The results show a region of increased water vapor pressure anomalies within the typhoon circulation, extending from the surface up to 16 km in altitude within 600 km of the storm center, and from 1,5 km to 16 km in the area 600 -1200 km from the center. The water vapor pressure anomaly reaches its maximum near the storm center and gradually decreases with distance. Within 200 km of the center, the peak anomaly is found at altitudes between 2 km and 3 km, with values exceeding 2,5 hPa. In the 500 - 600 km range from the center, the maximum anomaly

decreases to around 1 hPa. In the outer region between 700 km and 1200 km from the storm center, the water vapor pressure anomaly is mostly below 0,5 hPa.

3.3.4. Characteristics of atmospheric refractive index field

The results show that the anomaly trend of the atmospheric refractivity index is quite similar to the trend of water vapor pressure anomalies. The increase in refractivity index within 600 km of the typhoon center is greater than in regions beyond 600 km. Within the 0-600 km range from the typhoon center, the region of increased refractivity anomalies is located in the layer from the surface up to approximately 10 km in altitude. The maximum increase in refractivity index reaches 10 units in the layer between 2 km and 3 km altitude within 200 km of the typhoon center.

CHAPTER 4. CHARACTERISTICS OF TOTAL PRECIPITABLE WATER IN THE NGHIA DO AREA USING GLOBAL NAVIGATION SATELLITE SYSTEM DATA AND MODEL RESULTS

4.1. Evaluation of total precipitable water data calculated from GNSS data in Nghia Do area

The values of mean error (ME), root mean square error (RMSE), and correlation coefficient (R) between total precipitable water (TPW) calculated from GPS data and the TPW product from AERONET data are 0,68 mm, 2,05 mm and 0,988, respectively. The ME, RMSE and correlation coefficients between the total precipitable water calculated from GNSS data and from radiosonde data are -3,01 mm, 3,24 mm and 0,996, respectively. When compared with the WRF model simulation data, the ME, RMSE, and correlation coefficient are -2,12 mm, 3,08 mm and 0,984, respectively (Table 4.1). These comparison results demonstrate a high level of agreement between TPW calculated from GPS data at the Nghia Đò station using the CSRS-PPP tool and TPW products from AERONET and radiosonde data. The comparisons provide strong evidence that applying the CSRS-PPP technique to calculate TPW from GPS data at the Nghia Đò station yields reliable results.

Table 4.1. Comparison between total precipitable water calculated from GPS data (TPW_GPS) and from Aeronet data (TPW_AER), radiosonde data (TPW_RS).

	ME (mm)	RMSE (mm)	R
TPW_GPS and TPW_AER	0,68	2,05	0,988
TPW_GPS and TPW_RS	-3,01	3,24	0,996
TPW_GPS and TPW_WRF	-2,12	3,08	0,984

4.2. Characteristics of total precipitable water in Nghia Do area, Hanoi.

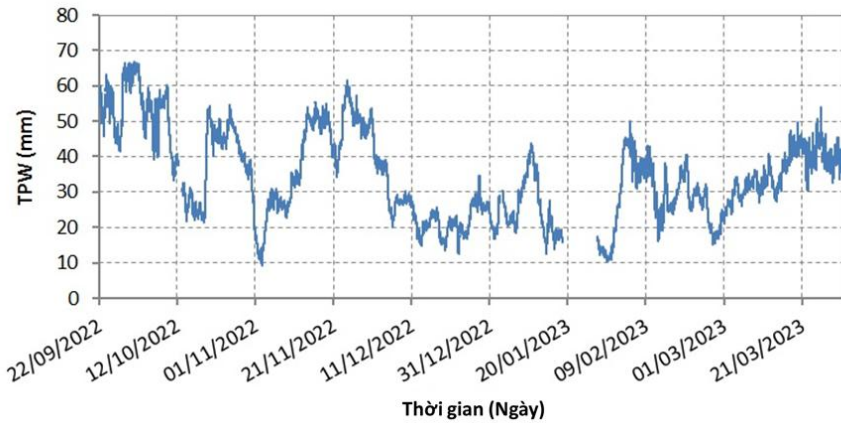


Figure 4.1. Temporal variation of total precipitable water (TPW) during the period from September 22, 2022 to March 31, 2023 at Nghia Do station

The GNSS data were continuously observed at the Nghia Do station (Hanoi) during the period from September 22, 2022, to March 31, 2023. During this time, GNSS data were collected for a total of 183 days. The results of the total precipitable water (TPW) calculations at a 1-minute resolution are presented in Figure 4.1. TPW values ranged from 9,3 mm to 66,8 mm. The results also indicate that the variation trend of TPW closely follows the trend of the zenith wet delay (ZWD). Overall, the TPW trend shows lower values during December and January compared to other months.

Analysis of the variation in monthly average total precipitable water (TPW) values calculated from GPS data during the period from

October 2022 to March 2023 at the Nghia Do station shows that January recorded the lowest value, reaching 22,73 mm (Figure 4.2). The result indicating that January has the lowest average TPW at the Nghia Do station is consistent with previous research findings.

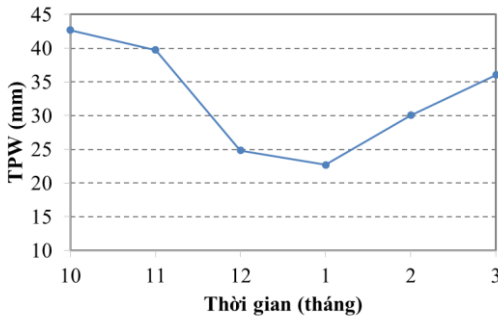


Figure 4.2. Temporal variation of monthly average total precipitable water (TPW) during the period from October 2022 to March 2023 at Nghia Do station

An examination of the diurnal variation of total precipitable water (TPW) during this period shows that TPW reaches two daily maximums and two minimums. The maximum values occur at 10:00 AM and 10:00 PM (local time), while the minimum values occur at 4:00 AM and 4:00 PM (local time).

The results of the daily average variation show that during the study period, the daily average value of total precipitable water from GNSS data (TPW_GPS) fluctuated significantly between days in October and early November. The daily average TPW in December and January was lower compared to the other months. The daily average TPW_GPS values ranged from 11,6 mm to 64,7 mm. When combined with daily rainfall data, it was observed that TPW_GPS values on rainy days were generally higher than those on surrounding dry days.

During the study period, Hanoi was affected by 15 cold air. Analyzing the changes in daily average temperature clearly shows that during each cold air incursion, the daily average temperature dropped sharply (Figure 4.3). The magnitude of the temperature decrease depended on the intensity of the cold air and the local environmental conditions at the station. The daily average temperature could drop significantly (by about

12,8°C on November 30, 2022) or more slightly (by about 0,4°C on December 4, 2022).

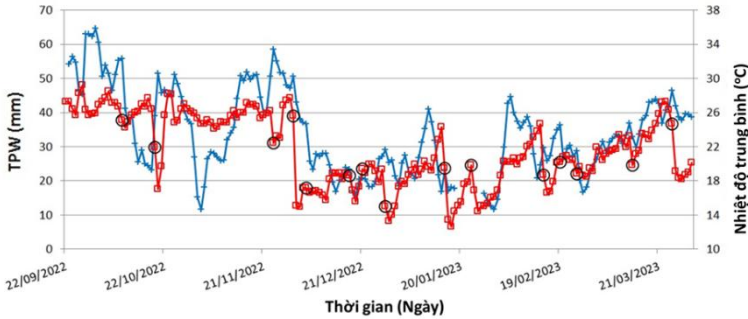


Figure 4.3. Variation of the daily mean value of TPW calculated from GPS data (TPW_GPS) (+, blue) and the daily mean value of temperature at Nghia Do station (square, red). The black circle shows the day when cold air affects the Hanoi area.

The analysis of air temperature variations observed at the Nghia Do station shows that, in several cases, a rapid decrease in air temperature occurred at a specific time of day when a cold air began to affect the Hanoi area. These cases include the cold air on 09/10/2022, 30/11/2022, 28/12/2022, 14/02/2023, 24/02/2023 và 25/03/2023. In these cases, we can use changes in air temperature at the station to determine the time when the cold air begins to affect the station area. Analysis of the variation in total precipitable water (TPW) shows that the TPW tends to increase and then decrease on the day when cold air begins to affect the Hanoi area. The time when the total precipitable water (TPW) reaches its peak is close to the time when the air temperature drops rapidly. In cases where cold air affects the Hanoi area but no rapid temperature change is observed, the variation in total precipitable water (TPW) is still similar to cases with a rapid temperature drop. The total precipitable water (TPW) tends to increase and then decrease during this day. WRF model simulation results also indicate the same trend of TPW increasing and then decreasing during cold air affecting Hanoi. However, the decrease in TPW appears earlier in the model simulation compared to the GNSS-derived TPW data.

To provide an overview of the variation in total precipitable water (TPW) under the influence of approaching cold air affecting the station area, the researcher calculated the average air temperature and TPW values across 14 cold air events. The results show that the time when the average TPW reaches its peak closely coincides with the onset of a rapid drop in average air temperature. On average, the temperature decreased by approximately $4,5^{\circ}\text{C}$ within 12 hours after the TPW peak. Additionally, the average TPW increased by about 5,25 mm during the 12 hours before the arrival of the cold air began influencing the station area. The average TPW decreased by approximately 5,9 mm in the 12 hours after the cold air began influencing the station area. According to Pham Ngoc Toan and Phan Tat Dac (1993), a tropical front forms when a wedge of high pressure from the polar region advances southward into tropical air. In this scenario, the cold air acts like a wedge that moves in and pushes back the warm, moist tropical air, forcing it to ascend, which leads to the formation of dense clouds along the boundary between the two air masses. The upward motion of air ahead of the cold front could be the reason for the increase in TPW before the cold air reaches the station.

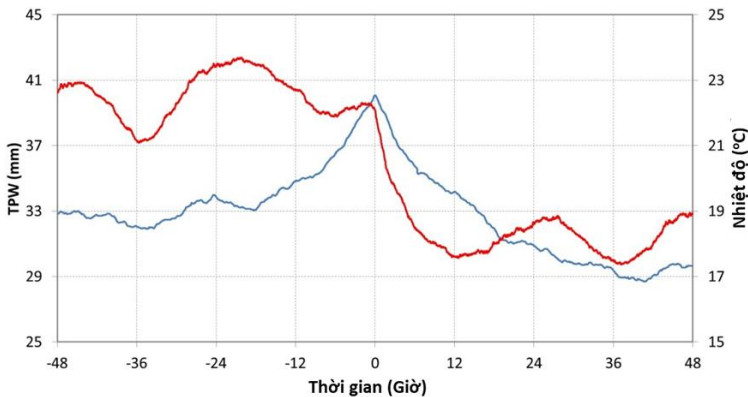


Figure 4.4. Variation of TPW (blue line) and air temperature (red line) averaged over 14 cold air waves over a period of ± 48 hours from the time TPW reached its maximum value.

The results above indicate that when a cold air outbreak affects the station area, the variation in total precipitable water (TPW) exhibits distinct

characteristics: TPW increases as the cold air approaches the station and then decreases sharply after the cold air passes through. Given this pattern, TPW can potentially be used as an indicator to determine the timing of a cold air outbreak's impact on the station area. However, it is important to note that when using TPW data to identify the arrival of cold air, the influence of other mesoscale systems must be excluded for example: tropical storms, tropical depressions, and disturbances in the easterly wind belt. These systems can significantly affect local weather conditions.

CONCLUSION AND RECOMMENDATIONS

CONCLUSION

The research project successfully applied GNSS data, GPSRO data, and numerical models to study and evaluate several atmospheric parameters in specific regions of Vietnam. Based on the results presented above, several conclusions can be drawn as follows:

1. Temperature, relative humidity, and atmospheric refractivity index data from the wetPf2 dataset show good agreement with radio occultation data over Vietnam and neighboring areas. The correlation coefficients between the two data sources range from 0,86-0,93, 0,63-0,76, 0,76-0,87 for temperature, relative humidity and atmospheric refractive index, respectively. The wetPf2 data also align well with WRF model simulation results under storm conditions. These findings confirm that the wetPf2 dataset is a reliable source of independent atmospheric observations and can serve as a valuable supplement to radiosonde data for atmospheric research and operational weather forecasting in Vietnam and neighboring areas.

2. In the Hoang Sa and Truong Sa islands, the annual temperature variation amplitude is greater in the boundary layer than in the free atmosphere. The annual temperature variation amplitude in the Hoang Sa islands reaches $\sim 5^{\circ}\text{C}$, which is higher than that of the Truong Sa islands ($2,2^{\circ}\text{C}$). In contrast, the annual variation amplitude of relative humidity is small in the atmospheric boundary layer, while it is significantly larger in

the free atmosphere.

3. The structure of atmospheric fields in typhoons over the East Sea and neighboring areas, derived from wetPf2 data, clearly shows a warm temperature anomaly near the typhoon center, extending from an altitude of 2,5 km to 15 km, which is associated with latent heat release due to condensation. The cold anomaly region at altitudes above 16 km is associated with cooling processes caused by evaporation. The region of increased relative humidity anomaly exists within the 5 km to 12,5 km layer, within a 600 km radius from the storm center, and is associated with strong convective activity near the storm center that transports moisture from lower levels to the upper atmosphere. The region of increased water vapor pressure and atmospheric refractive index anomalies is located at lower altitudes, within the 2 km to 3 km layer near the typhoon center.

4. The results have confirmed that the precipitable water vapor (TPW) calculated from GNSS data with a 1-minute resolution is reliable and consistent with other data sources. The RMSE (correlation coefficient) between the total precipitable water (TPW) derived from GNSS data and that from AERONET, radio occultation, and model simulation data are 2,05mm (0,988), 3,24mm (0,996) and 3,03mm (0,984), respectively.

5. The variation of total precipitable water (TPW) shows a diurnal pattern with two maxima occurring at 10:00 and 22:00 and 2 minima at 4:00 and 16:00. Total precipitable water tends to increase before the cold air mass moves toward the station. After that, it decreases once the cold air mass passes through the station area. This variation in total precipitable water can be used as one of the indicators to determine the time when the cold air begins to affect the station area.

RECOMMENDATIONS

GPSRO and surface GNSS data have been confirmed as reliable sources for use in atmospheric, weather, and climate research, as well as in operational forecasting in the Vietnam region. In this dissertation, the use of COSMIC-2 data to study the structural characteristics of meteorological fields in typhoons was only applied for the 2020 typhoon season, which

included a limited number of storms and therefore may not fully represent other typhoon seasons. Data assimilation into models has not yet been implemented. Future studies will focus on using COSMIC-2 and other GPSRO data to analyze meteorological field characteristics for different typhoon seasons in the East Sea, analyze characteristics of other atmospheric fields such as atmospheric boundary layer thickness, changes in tropospheric top height, as well as research on assimilating this data into the WRF model to forecast storm trajectory, intensity and rainfall in typhoons.

The use of GNSS data to calculate high-resolution total precipitable water (TPW) has demonstrated its potential for monitoring climate change. In this dissertation, the data was used to analyze the characteristics of precipitable water vapor associated with cold air, however, the number of cold air events was limited, and these findings are preliminary, so further studies using longer data series are necessary, potentially including other extreme weather events such as heavy rainfall. In addition, it is also necessary to focus on assimilating GNSS data into the WRF model for simulating and forecasting rainfall in the Hanoi area.

LIST OF THE PUBLICATIONS RELATED TO THE DISSERTATION

- 1) **Khuong Le Pham**, Anh Xuan Nguyen, Hiep Van Nguyen, Son Hai Hoang, Vinh Nhu Nguyen, Thang Van Vu. *Application of WetP_{f2} Data for Investigating Characteristics of Temperature and Humidity of Air Masses over Paracel and Spratly Islands*. Advances in Meteorology, 2024, Vol 2024.
- 2) **Pham Le Khuong**, Nguyen Xuan Anh, Hiep Van Nguyen, Hoang Hai Son, Nguyen Nhu Vinh, Bui Ngoc Minh. *Precipitable Water Characterization Using Global Navigation Satellite System Data: A Case Study in Nghia Do Area, Vietnam*. Vietnam Journal of Earth Sciences, 2024, Vol 46, No. 1, pp 82-99.